Journal of Computational Science 53 (2021) 101374

Contents lists available at ScienceDirect

Journal of Computational Science

journal homepage: www.elsevier.com/locate/jocs

Diagnosis of lung cancer using hybrid deep neural network with adaptive sine cosine crow search algorithm

Surendar P. [a,*], Ponni Bala M. [b]

[a] Department of ECE, Vivekanandha College of Engineering for Women, Tiruchengode, 637205, India
[b] Department of EIE, Kongu Engineering College, Erode, 638060, India

ARTICLE INFO

Keywords:
Lung cancer
Deep neural network with adaptive sine cosine crow search
Grey-level run length matrix
Binary grasshopper optimization algorithm
Masientropy based multilevel thresholding using salp swarm algorithm
Fast non local means filter

ABSTRACT

Lung cancer is a leading cause of cancer related deaths in all around the world. The identification of lung nodules is the significant step in the diagnosis of earlier lung cancer which can develop into a tumor. In the lung disease analysis, valuable information is provided by the Computed Tomography (CT) scan. The key objective is to find the malignant lung nodules and categorize the lung cancer whether it is benign or malignant. In this paper, propose a diagnosis of lung cancer using hybrid deep neural network with adaptive optimization algorithm. Initially, the preprocessing stage is performed using the fast non local means (FNLM) filter. For the segmentation process, the Masi entropy based multilevel thresholding using salp swarm algorithm (MasiEMT-SSA) is used to segment the cancer nodule from the lung images. Using the grey-level run length matrix (GLRLM), different features are mined in the feature extraction. The binary grasshopper optimization algorithm (BGOA) is applied to select the optimum features for the feature selection (FS) process. Then the selected features are classified using the hybrid classifier named as deep neural network with adaptive sine cosine crow search(DNN-ASCCS) algorithm. The proposed hybrid classifier accurately detects the lung cancer. The proposed (DNN-ASCCS) is implemented by MATLAB using the Lung Image Database Consortium and Image Database Resource Initiative (LIDC-IDRI) datasets. The different performance metrics are evaluated and related to the existing classifiers and different state-of-art approaches. The simulation outcomes verified that the developed scheme is achieved a high classification accuracy (99.17 %) compared to other approaches.

1. Introduction

In bio-medical applications, image processing (IP) methods are generally applied [1]. Digital image processing plays a significant role in medical diagnostics [2]. Bio-medical image processing refers to the provision of digital image processing for biomedical sciences. Biomedical imaging is a dominant tool is used to envisioning the inner structures of the body and its infections [3].To enhance the accuracy of detection approach, the real-time processing is a significant step in bio-medical field. In addition, the bio-medical imaging is used to analyse the fatal diseases like cancer in early stages which leads to more active treatments [4].

The most dangerous disease is cancer that causes deaths in humans [5]. Using the progressive methods, the various types of cancer like lung cancer [6], breast cancer [7], prostate cancer [8] and colon cancer [9] are identified. The early diagnosis of cancer plays a significant task to avoid cancer cells from spreading and multiplying [10]. Cancer patients have more treatment options and a far great chance of survival when cancer is detected at its initial state. For the cancer analysis, a different imaging modalities such as CT, chest X-ray, magnetic resonance imaging (MRI) and positron emission tomography (PET) are utilized.

The CT scanner occupied the several detailed images and these images are merged by the computer into image of slices in which some nodules are round figured but not accurately malignant [11]. Therefore, the tumor analysis for a radiologist is a serious and time consuming task. CT image is more sensitive to discover the tumor size. In the early detection of lung cancer, the Computer Aided Diagnosis (CAD) has been referred a new step [12]. To improve the specificity, sensitivity, accuracy and cost-effectiveness of lung cancer, the CAD system is used [13]. To highlight the visible region that are affected by the disease, CAD system utilizes the digital images [14]. For the lung cancer prediction, the researchers have been developed the numerous CAD systems [15]. By deliberating the system-generated outcome with the clinical analysis, such systems support the radiologist to create a final decision.

* Corresponding author.
E-mail addresses: surenecemkce@gmail.com (S. P.), ponnibala@kongu.ac.in (P.B. M.).

https://doi.org/10.1016/j.jocs.2021.101374
Received 10 January 2021; Received in revised form 24 March 2021; Accepted 13 April 2021
Available online 3 May 2021
1877-7503/© 2021 Elsevier B.V. All rights reserved.

Lung cancer is a most common cancer in both men and women [16]. A disease of abnormal cells growing and multiplying into a tumor is termed as lung cancer. Through the blood stream that surrounds the lung tissue, the cancer cells can spread from the lungs. Due to the natural flow of lymph, the cancer cells frequently spread in the direction of the center of the chest. The spreading of cancer cells are prevented by the prior analysis of lung cancer [17]. By the IP methods such as pre-processing, segmentation [18], feature extraction [19], and classification [20], the CAD system can inspect more collection of CT images for improved and early analysis of lung cancer. Machine learning (ML) and IP schemes are executed to find and categorize the lung tumor. Therefore, early diagnosis of the disease plays a major role to avoid severe progressed stages and to decrease its ratio of distribution.

The measurements of the human body on various scales is termed biomedical images. In a broad variation of imaging modalities, these images are originated and it measure a physical property of the human body. For analysis, these images are taken by domain scientists and it have a high impact on decision making of surgeons. The diagnosis of early lung cancer can improve the survival chance between people. CAD plays a major role in the earlier analysis of lung tumor. Moreover, it covers a combination artificial intelligent (AI) and IP methods to find the abnormalities in medical images. In addition, for a quality performance, it improving medical clarification in the detection process.

The contributions can be shortened as trails:

- To find the lung cancer at early stage
- To achieve more accurate result by using various image processing techniques
- To present CAD system based hybrid DNN with adaptive optimization algorithm
- To get better classification accuracy by extracting the optimal features under the efficient feature extraction and feature selection approaches.
- To minimize the error during classification process
- To minimize the execution time

The rest of the paper is defined as trails: the following section describe the recent related works. Section 3 provide the developed approach for detection of lung cancer, the simulation outcomes are explained in the fourth section and fifth section mentioned the conclusion and future scope.

2. Related works

The recent literature works related to lung cancer detection are as follows:

The diagnosis of earlier lung tumor was developed by Arulmurugan and Anandakumar [21] by ANN (Artificial Neural Network) and Wavelet feature descriptor (WFD) classifiers. From the GLCM (Gray level co-occurrence matrix) of Daubechies WT (wavelet transform), the WFD were estimated. By the feed forward back propagation (FWBP) and feed forward neural network (FFNN), The NN classifier was intended through deliberating the training functions. The results proved that the FWBP has provide the good classification outcomes compared to other networks.

For a lung cancer diagnosis, a survey on different IP methods was presented by Ayshath et al. [22] using the CT scan images. This review analysed the numerous image development schemes like Weiner filter (WF), Gabor filter (GF), Auto enhancement and median filter (MF). From this analysis, the GF produces the superior outcomes. In the process of segmentation, the Ostu's thresholding approach is utilized to extract the object from its background. For feature mining process, the binarization and masking were applied. SVM (Support Vector Machine) classifier is utilized for the classification process. From the feature mining method, the eccentricity and Area features are estimated and these features are considered as the classifier input. Classifier identifies the lung nodule in CT image whether it is benign or malignant.

For the lung tumor diagnosis, the circulating MicroRNA (miRNA) biomarkers was introduced by Haixin et al. [23]. For the identification of lung tumor, the survey was conducted in East Asia on the analytical value of miRNA markers. The performance measures such as accuracy, sensitivity, specificity were investigated based on population characteristics and study design. Finally, the analytical values of circulating miRNAs in East Asia were compared with the Western populations. Among both the populations, 44 miRNAs were reported. It is evident that circulating miRNAs with genetic and epigenetic biomarkers given promising results for identifying the prior non-invasive lung tumor.

An automatic computer-aided lung tumor analysis approach was developed by Ananya and Swanirbhar [24] to identify malevolent nodules. This approach covers the different IP methods such as image acquisition, pre-processing, detection of nodule, segmentation and post-processing using LIDC-IDRI database. Median filtering based smoothening, pre-processing with histogram equalization, edge detection and region of interest extraction using morphological operations were performed.

A novel functional test named Liquid ImmunoBiopsy was introduced by Yochai et al. [25]. This approach measure the metabolic activity profiles (MAPs) of immune system and acidification stages of extra cellular surroundings. ML tools were used to analyse the MAPs for cancer diagnosis. A multivariable prediction system was utilized to distinguish lung tumor and blood samples. The extracellular acidity was measured using commercial fluorescence plate reader. The 20-fold cross validation scheme was developed. At first, to mine the significant classifier features, the raw MAP test data are examined. Then the mined features are taken as the input to the ML system.

Zhang et al [41] suggested a standard 8-layer CNN, then integrated two improvement techniques are batch normalization (BN) and dropout (DO). Then rank-based stochastic pooling (RSP) to substitute the traditional max pooling. This resulted in BDR-CNN, which is a combination of CNN, BN, DO, and RSP. This BDR-CNN was hybridized with a two-layer GCN, and yielded our BDR-CNN-GCN model.

Wang et al [42] proposed CNN employed several new techniques such as rank-based average pooling and multiple-way data augmentation. On the other hand, relation-aware representations were learnt from graph convolutional network (GCN). Deep feature fusion (DFF) was developed in this work to fuse individual image-level features and relation-aware features from both GCN and CNN, respectively. The best model was named as FGCNet.

2.1. Problem statement

Medical images are inherent in nature, so the segmentation of image is a tedious and interesting task. Due to intersecting intensity spreading of strong tissues and tumor, different approaches are introduced in the literature and it have encountered with only restricted success. The lung tumor identification needs the more collection of data. In every year, the number of recorded cancer patients is growing significantly. Still, there are number of unidentified types of tumors recorded. Previous researches include analysing lung cancer with general IP methods namely image acquisition and development, segmentation and feature extraction. In this work, we developed and assessed extra feature selection and feature classification method to diagnose the lung cancer. The feature

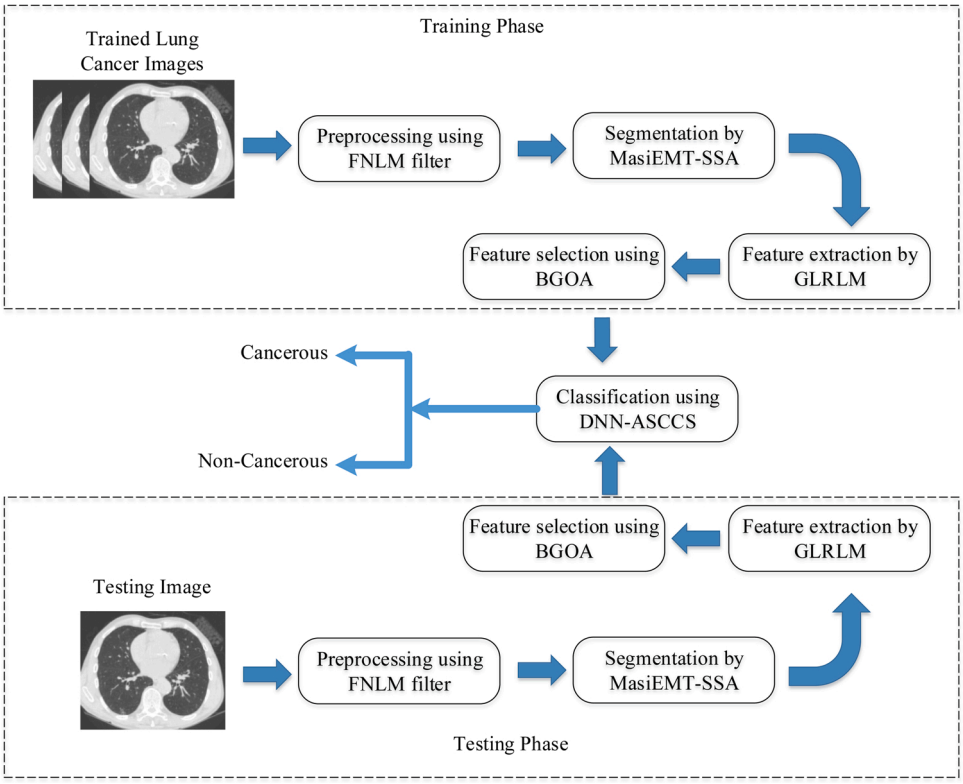


Fig. 1. Proposed work.

classification process is obtained using a hybrid classifier that identifies the weights and biases arbitrarily between input and hidden neurons. Ordinary deep learning algorithms learn only these weights by providing the solution to the linear model. Nevertheless, this new concept, delivers improved performance in simplification, and its training time is extremely effective.

3. Proposed methodology

In the world, the most dangerous disease is lung cancer. But, the early prediction and cure can save life. This disease shows symptoms in final stage for this reason the prediction of lung tumor is challenging task. By the earlier prediction and cure of the disease, the probability and mortality rate can be decreased. The proposed scheme consist of following stages: pre-processing, segmentation, feature extraction, feature selection and classification as shown in Fig. 1.

Initially an input lung cancer image is acquired from LIDC-IDRI database. Next the image is pre-processed and filtered. Here, the image is converted into gray scale image and to remove the noise using a filter. Here, the filtering technology named FNLM filter is used to eliminate impulsive noise presented at the images. In addition to that segmentation is done with MasiEMT-SSA. Here based upon the histogram value, the image segmented and this will improve the segmentation accuracy. In the next step, features are mined using GLRLM. Then the significant features are carefully chosen using BGOA. Finally this selected feature is given to the Hybrid classifier namely DNN-ASCCS for classification also this will give the severity of the tumour.

3.1. Preprocessing

The preprocessing is a most significant step in lung cancer detection. It is essential to enhance the detection accuracy and to remove the particular regions of CT image such as background and surrounding issues or vessels. Initially, the images are transformed into the gray scale images. Then the FNLM filter is utilized to remove the noise. The mathematical model of FNLM is described in the following section.

3.1.1. FNLM filter for noise reduction

FNLM [26] is applied to eliminate the noise from the images. It is related to the neighborhood filter that mines an average value of neighbouring pixels to a central pixel. Using the spatial data across the image, the FNLM filter is achieved the pixel value.

For the NLM, the weights are calculated which only use pixel information to measure the similarity between a central region patch and its neighboring patches. In this paper, the proposed method is to combine the advantages of the Non Local Means algorithm and the bilateral filter with added texture information as weights. For this reason, the FNLM filter is differs significantly.

According to the structural similarity of neighbouring pixels, the weights are computed. The high weight is assigned once the similarity of gray-level in the neighbouring pixel is high. The FNLM filter is represented as:

$$NL\,[I]\,(m) = \sum_{n \in I} w(m,\ n)\ I(n) \tag{1}$$

Where the weight is denoted as $w(m,\ n)$ for every single region and fulfils $0 \le w(m,\ n) \le 1$ and $\sum_{n \in I} w(m,\ n) = 1$. For each region, the weight can be computed by:

$$w(m,\ n) = \frac{1}{Z(m)} \sum_{n} e^{\frac{-G_\sigma(\lambda)\ \|I(m+\lambda)-I(n+\lambda)\|_2^2}{d^2}} \tag{2}$$

Where d changes the weight for every area and $\|I(m+\lambda) - I(n+\lambda)\|_2^2$ is a value accomplished by estimating the alteration in intensity among adjacent pixels.

Algorithm 1:

Pseudo code of FNLM filter

Input: Original input image and size of the image
Output: Filtered image
Step 1: Pixel values are computed
Step 2: The differences in intensity among adjacent pixels are computed by $\|I(m+\lambda) - I(n+\lambda)\|_2^2$
Step 3: for each region weight value is computed Using Eq. (2)
Step 4: image is filtered using Eq. (1)

3.2. Segmentation

The process of segmentation is a significant step in the IP. Segmentation is a procedure of dividing the image into sub-regions. It is generally perform to offer a difference between various parts of an image. The main aim of this process is to make things easier and modify the depiction of the image. Therefore, that it could become more important and easier to analyze. In this work, a MasiEMT-SSA is used for the segmentation process.

3.2.1. MasiEMT-SSA

For an image segmentation process, a multilevel thresholding (MT) method is established that uses the Masi entropy as an impartial function. The complexity of MT is growths quickly with growing number of thresholds. Therefore, the SSA is employed to adjust the threshold process and to decrease the computational complexity (CC) involved in MT.

To implement the segmentation of an image, the MT [27] employs large number of thresholds. Consider a set of m number of thresholds $\{t_1,\ \ldots,\ t_m\}$ for the segmentation of an image. These thresholds are utilized to divide the image into $m+1$ classes. $C_0,\ C_1,\ \ldots.,\ C_m$ covering the pixels with the gray levels in the range $[0,\ t_1]$, $[t_1+1,\ t_2]$, $\ldots.$, $[t_m+1,\ L-1]$ correspondingly. The Masi entropy for MT is given as:

$$S_r(I|\{t_1,\ \ldots,\ t_m\}\ ) = S_r(C_0) + S_r(C_1) + \ldots + S_r(C_m) \tag{3}$$

Where,

$$\begin{aligned} S_r(C_0) &= \left(\log\left(1-(1-r)\sum_{i=1}^{t_1}\left(\frac{h_i}{\omega_0}\right)\log\left(\frac{h_i}{\omega_0}\right)\right)\right) \Big/ (1-r) \\ S_r(C_1) &= \left(\log\left(1-(1-r)\sum_{i=t_1+1}^{t_2}\left(\frac{h_i}{\omega_1}\right)\log\left(\frac{h_i}{\omega_0}\right)\right)\right) \Big/ (1-r) \\ &\vdots \\ S_r(C_m) &= \left(\log\left(1-(1-r)\sum_{i=t_m+1}^{L-1}\left(\frac{h_i}{\omega_m}\right)\log\left(\frac{h_i}{\omega_1}\right)\right)\right) \Big/ (1-r) \end{aligned} \tag{4}$$

Here, $\omega_0 = \sum_{i=1}^{t_1} h_i,\ \omega_1 = \sum_{i=t_1+1}^{t_2} h_i,\ \ldots,\ \omega_m = \sum_{i=t_m+1}^{L-1} h_i$ are the class probabilities of the classes $C_0,\ C_1,\ \ldots.,\ C_m$ respectively. In the Eq. (3), by maximizing the Masi entropy function the optimum set of thresholds $\{t_1,\ \ldots,\ t_m\}$ is establish.

The key motivation of SSA [28] mimics the crawling behaviour of salps. It is capable to enhance the initial random solutions efficiently and converge in the direction of the best value. In this algorithm, the population is divided into two groups such as leaders and followers. The leader salp is located in the front of the chain and the remaining salps are followers. The leader is guide the swarm and the followers are follow each other. In the SSA, the potential solutions are signified by a salps. The locations of the salps are the thresholds. By altering their corresponding location vectors, the salps are travel in the n-dimensional search space. By randomly initializing the locations of the salps, the algorithm starts in the search space as:

$$P = round\ \ (rand\ \ (noS,\ \dim).^{*}(ub - lb) + lb\ ) \tag{5}$$

Here, the number of salps is denoted as noS, the number of thresholds is defined as dim, and the upper and lower bound of the thresholds are represented as ub and lb.

The fitness of each salp is estimated through the Masientropy function which obtained by Eq. (3). The position of the leader and followers are updated by:

$$x_j^1 = \begin{cases} F_j + c_1\left(\left(ub_j - lb_j\right)c_2 + lb_j\right) & c_3 \ge 0 \\ F_j - c_1\left(\left(ub_j - lb_j\right)c_2 + lb_j\right) & c_3 < 0 \end{cases} \tag{6}$$

$$x_j^i = \frac{1}{2}\left(x_j^i + x_j^{i-1}\right) \tag{7}$$

Here, the position of the leader is denoted as x_j^1, the position of the food source is defined as F_j, and the location of i^{th} follower salp is denoted as x_j^i in j^{th} dimension. $c_1,\ c_2$ *and* c_3 are the arbitrary numbers. According to the food source, the leader updates their position. The factor c_1 is the best significant constraint because it equilibriums exploitation and exploration stage is given by:

$$c_1 = 2e^{-\left(\frac{4l}{L}\right)^2} \tag{8}$$

Where, the present iteration is denoted as l and the maximum number of iteration is defined as L. This entire procedure is frequent for a maximum number of iterations. The finest location of the salp provides the preferred set of optimum thresholds.

Algorithm 2:

Pseudo code of MasiEMT-SSA

Randomly initialize the location of salps using Eq. (5)
for$(i = 1:\ \ Max_Iteration)$
for each salp
Compute the fitness using Eq. (3)
end for
Compute the c_1 value using Eq. (8)
for each salp
if$(i == 1)$
Update the location of leader using Eq. (6)
else
Update the location of followers using Eq. (7)
end if
end for
end for

3.3. Feature extraction

The process of feature mining plays avital part in the discovery of lung tumour. It is the procedure of the certain features are extracted within an image for further processing the lung cancer image. Using the GLRLM method, the dissimilar kinds of features are mined from the segmented image.

3.3.1. GLRLM

The GLRLM [29] approach is utilized to extracting the higher order numerical texture information. By re-quantization prior to the growth of the matrix, the quantity of gray levels G is reduced in the image. The features of Run Length Nonuniformity (RLN), Long Run High Gray-Level Emphasis (LRHGLE), Low Gray-Level Run Emphasis (LGLRE), Long Run Emphasis (LRE), Gray-Level Nonuniformity (GLN), Run Percentage (RP), Long Run Low Gray-Level Emphasis (LRLGLE),High Gray-Level Run Emphasis (HGLRE), Short Run Low Gray-Level Emphasis (SRLGLE), Short Run High Gray-Level Emphasis (SRHGLE), and Short Run Emphasis (SRE) are extracted using the GLRLM approach. The GLRLM is established as:

$$K(\theta) = (r\ \ (u,\ v)/\theta), \quad 0 \le u \le N_r, \quad 0 \le v \le K_{\max} \tag{9}$$

Where, the maximum length is denoted as $K_{\max}$, the maximum gray level is represented as N_r and $u,\ v$ is a matrix size values.

3.4. Feature selection (FS)

Feature selection is a noteworthy task which decreasing the quantity of features by eliminating redundant, inappropriate and noisy information through sustaining the adequate level of classification accuracy. In this work, the BGOA is used to choose the optimal features from the feature extraction process.

3.4.1. BGOA

Under the specific conditions, the Grasshoppers are considered a pest. The key feature of these insects is connected to their movement. In a larval state, its movement is slow as compared to the huge and rapid movements of the adults. The movement of the grasshoppers can be given as:

$$X_i^d = c_1\left(\sum_{j=1,\, j\neq i}^{N} c_2 \frac{ub_d - lb_d}{2} s\left(\left|x_j^d - x_i^d\right|\right)\frac{x_j - x_i}{d_{ij}}\right) + \widehat{T}_d \tag{10}$$

Here, the upper and lower bound are defined as ub_d and lb_d in the D^{th} measurement, $\widehat{T}_d$ is the significance of the D^{th} size in the goal, $s(d) = fe^{\frac{-d}{l}} - e^{-d}$ and c is a reducing factor to reduce the ease region, attraction and repulsion area. The factor c is computed as:

$$c = c_{\max} - l\frac{c_{\max} - c_{\min}}{L} \tag{11}$$

Where, the maximum number of iteration is denoted as L, the current iteration is denoted as l, the $c_{\max}$, and $c_{\min}$ coefficients are 1 and 0.00001 respectively.

According to the current location, the finest grasshopper location and all other grasshoppers' location as in Eq. (10), every single solution is updated in the continuous version of GOA. The location vector covers only 1's and 0's in the binary space so the add operator cannot be utilized. Therefore, to change the continuous version of GOA to a binary, the transfer functions (TFs) are utilized. In GOA, the initial term of Eq. (10) is restructured in Eq. (12) as ΔX is similar to the velocity vector. TF is the best scheme to translate the procedure from continuous to binary without altering the construction. TF denotes the likelihood of modernising the binary solution's elements from 0 to 1. The likelihood of altering locations is depends on the step vector values in BGOA [30].

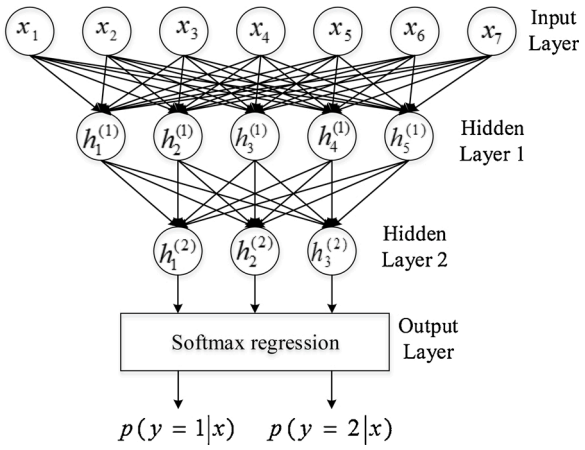


Fig. 2. DNN structure.

$$\Delta X = c_1\left(\sum_{j=1,\, j\neq i}^{N} c_2 \frac{ub_d - lb_d}{2} s\left(\left|x_j^d - x_i^d\right|\right)\frac{x_j - x_i}{d_{ij}}\right) \tag{12}$$

TFs are characterized into two types such as Sigmoidal (S-shaped) and Hyperbolic tan (V-shaped) based on their shapes. S-shaped function is a common TF is given by:

$$T(\Delta X_t) = \frac{1}{1 + e^{-\Delta X_t}} \tag{13}$$

Where ΔX signifies the velocity of a search agent at a particular repetition.

Based on the probability value which obtained from the Eq. (13), the location of the present grasshopper is improved by:

$$X_{t+1}^d = \begin{cases} 1 & if\ r_1 < T\left(\Delta X_{t+1}^d\right) \\ 0 & if\ r_1 \ge T\left(\Delta X_{t+1}^d\right) \end{cases} \tag{14}$$

Where the d^{th} measurement of the grasshopper is denoted as X_{t+1}^d in the following iteration, and r_1 is a arbitrary number that lies between 0 and 1.

V-shaped function is another TF is specified by:

$$T(\Delta X_t) = |\tanh\ (\Delta X_t)\,| \tag{15}$$

According to the likelihood value which gotten from the Eq. (15), the location of the present grasshopper is improved by:

$$X_{t+1}^d = \begin{cases} -X_t^d & r_2 < T\left(\Delta X_{t+1}^d\right) \\ X_t^d & r_2 \ge T\left(\Delta X_{t+1}^d\right) \end{cases} \tag{16}$$

Where, r_2 is a arbitrary number between 0 and 1.

To compute every solution, the fitness function is employed. The objective of the FS is to enhance the taxonomy accuracy and decreasing

the amount of nominated features. The solution with the smaller amount of features is chosen as the best solution. The classification error rate is used to decrease the amount of selected features. The fitness of the FS can be given as:

$$Fitness\ \ function = \alpha\gamma_R(D) + \beta\frac{|R|}{|N|} \tag{17}$$

Where the taxonomy error rate of the classifier is denoted as $\gamma_R(D)$, the number of features are denoted as $|N|$, the number of selected features are represented as $|R|$, α and β are the two parameters is used to reproduce the part of taxonomy rate and length of the subset. Here, $\alpha \in [0,\ 1]$ and $\beta = (1-\alpha)$.

Algorithm 3:

Pseudo code of the BGOA based feature selection

Input:
Number of Selected features
Number of population
maximum iteration
$c_{\max}$ and $c_{\min}$
Dimension of features
Output: optimal features (target)
Calculate each solution in the population
While the termination condition of the iteration is not satisfied ***do***
Update c using Eqn (11)
for each solution ***do***
Compute the fitness value using Eqn (17)
The distances among grasshoppers are normalized in [1, 4]
end for
The step vector of the current solution is updated using Eqn (12)
for $i = 1 : \dim$ ***do***
if $\Delta X > 0$ ***then***
X_{t+1}^{d} =target position
else
if $rand >= 0.5$ ***then***
Update the position using Eqn (14)
else
Update the position using Eqn (16)
end if
end if
end for
$t = t + 1$
end while
return Target (optimal features)

3.5. Classification

After the feature selection process, the chosen features are provided to the DNN classifier as the input. The softmax classifier is employed in the DNN output layer to identify the lung cancer. In this process, the entire network weights are updated using the ASCCS algorithm. Finally, the proposed hybrid classifier (DNN-ASCCS) effectively identify the lung cancer and it improves the classification accuracy.

3.5.1. DNN-ASCCS

The structure of DNN contains three layer such as input layer, output layer and hidden layers as shown in Fig. 2. The DNN is constructed with two hidden layers by the desired weight fitness for the mapping connection amongst the output and input data. During the training stage, the DNN is updating the weight values in the hidden layers using the ASCCS algorithm. The training iteration is increased so this NN continuously fits the decision boundary of the labelled training data. The two hidden layers are made to improve the training speed and classification accuracy.

The description is manipulated with one input layer, one output layer and two hidden layers. It is considered as the feasible network architecture since proper mapping is done between the data. In this study, the first hidden neuron will establish the connection with initial two lines and the last hidden neuron will establish the connection of last two lines. The expected decision boundary in order to segregate the classes has been implied. Since two connections has been made two hidden neurons has been used in this study to classify the classes. It has been depicted in DNN structure.

The entire amount of nodes in the hidden layer is estimated by:

$$n = \sqrt{r+s} + t \tag{18}$$

Where, the amount of hidden layer nodes is defined as n, r is the sum of input layer nodes, s is the sum of output layer nodes and t is the constant value in the range of [1,10].

In the hidden layer, an activation utility is employed for permitting the non-linear fitness ability. In this work, the sigmoid function is utilized as an activation utility which is given as:

$$S = \frac{1}{1+e^{-x}} \tag{19}$$

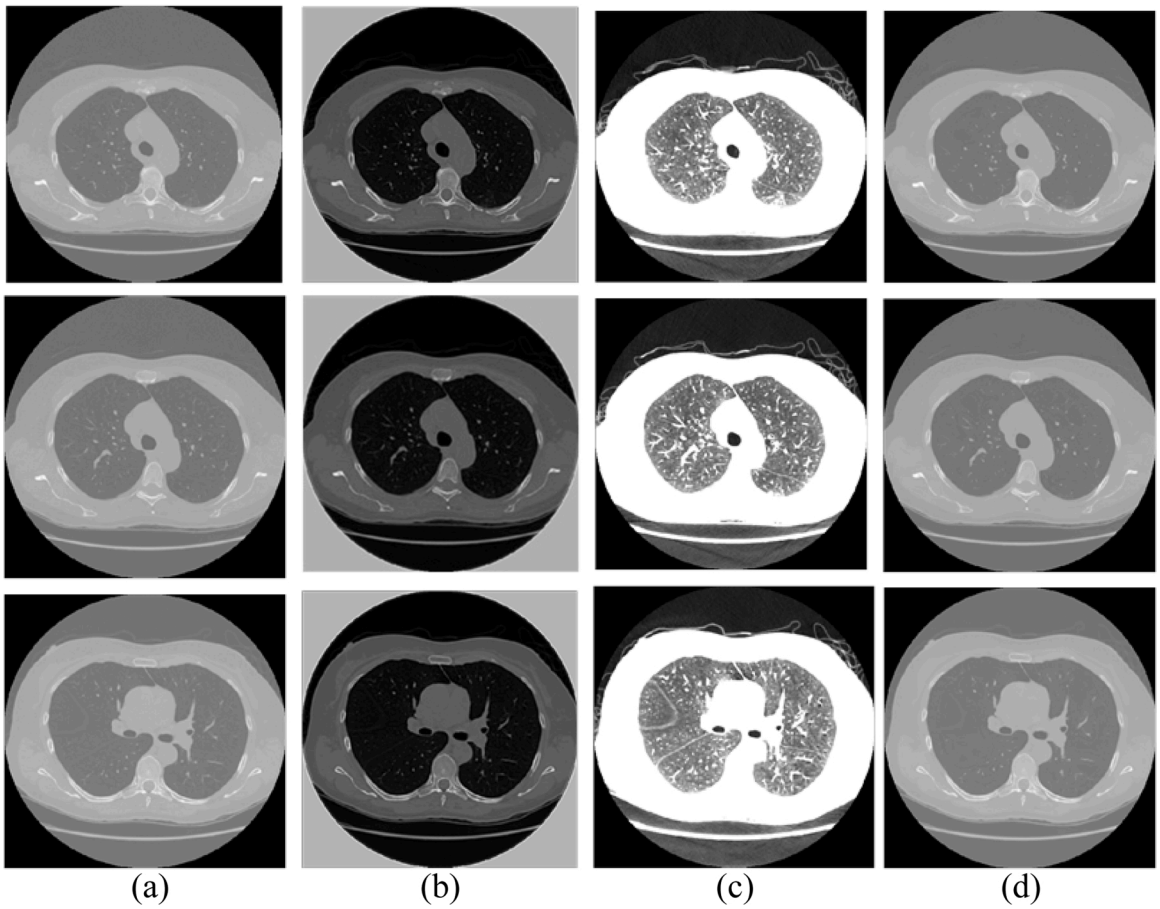


Fig. 3. (a) input images, (b) FNLM filter, (c) robust bilateral filter (d) rolling guidance filter.

Here, x is the input data of the system which is stimulated by the mapping function M_f is given as:

$$M_f = sigm\ (\alpha_i x + \beta_i) \tag{20}$$

Here, the weight matrix is signified as α and the bias among the hidden and the output layer is represented as β.

The supervised loss function is utilized to reason the depiction space of the hidden neurons to make parallel with humanoid data. The information in the data sample tags denotes the human ideas. Assume a theoretically categorized statistics model $(x,\ l)$. The loss form can be estimated by:

$$S(W_s,\ b_s;\ x,\ l) = \frac{1}{2m}\sum_{j=1}^{m}\left\|h_j(W_s,\ b_s;\ x) - l_j\right\|_2^2 \tag{21}$$

Where the subsets of biases are represented by W_s and b_s, the sum of neurons in the hidden layer is signified as m. For the preparation of testing and training, cross-entropy (CE) is considered as the DNN loss utility. The usage of CE losses significantly enhanced the enactment of the softmax and sigmoid yield designs. The loss of CE is computed by:

$$C_E = \frac{1}{n}\sum_{k=1}^{n}\left[Y_k \log \widehat{Y}_k + (1 - Y_k)\log(1 - \widehat{Y}_k)\right] \tag{22}$$

Where the training sample quantity is defined by n, the k^{th} actual output of the training set is denoted as Y_k, and the k^{th} expected output of the testing set is denoted as $\widehat{Y}_k$. The ASCCS process is utilized to compute the ideal weight value of DNN.

The main aim of ASCCS is to enhancing the fitness value of every single solution in the population. This procedure struggles the fitness to change in the direction of the finest solution by enhancing the values. It only needs alteration of the population dimension and the amount of repetitions which indications to the execution of the procedure is simple as its solution is improved by only one stage using a single expression. As compared to other optimization approaches, this algorithm has quicker convergence speed, low time and low computational complexity. The mathematical behaviour of this algorithm is described below:

The combination of sine cosine algorithm (SCA) [31] and crow search algorithm (CSA) [32] is named as SCCS. The benefits of the two algorithms are considered and use to design an effective hybrid algorithm which can perform very well compared to other algorithms. In this work, adaptive SCCS is termed as ASCCS is introduced for weight updation of DNN. Initially, the concept behind the CSA is considered in the ASCCS algorithm. CSA has two drawbacks. The first drawback is the search agent do not essentially track the finest solution. Second, in solution space, the search agents improve its location to an arbitrary place if $r_i \leq AP_i^t$ which suggestively reduces the CSA performance. Hence, to improve the effectiveness of the CSA, first it deliberated that every single solution improves its location depends on the finest solution location or depends on the arbitrarily preferred search agent location as follows:

$$X_i^{t+1} = \begin{cases} update\ the\ \ position\ based\ on\ the\ position\ of\ \ the\ best\ solution & r_1 < 0.5 \\ update\ the\ \ position\ toward\ a\ randomly\ chosen\ search\ agent & r_1 \geq 0.5 \end{cases} \tag{23}$$

Where r_1 is an arbitrary number between 0 and 1.In the SCCS algorithm, the inertia weight remains unchanged, which can certainly reason the population individuals to fluctuate in the later period of search. Therefore, the adaptive scheme of the inertia weight is introduced in the updation process which enhances the exploration stage. Every single search agent can select among CSA updation process or SCA movements to improve its location as trails:

$$X_i^{t+1} = \begin{cases} \xi(t).\ X_i^t + r_1 \times \sin(r_2) \times \left| r_3 P_i^t - X_i^t \right| & r_4 < 0.3 \\ \xi(t).\ X_i^t + r_1 \times \cos(r_2) \times \left| r_3 P_i^t - X_i^t \right| & 0.3 \leq\ r_4 \leq 0.6 \\ \xi(t).\ X_i^t + r_1 \times fl_i^t \times \left| m_i^t - X_i^t \right| & r_4 \geq 0.6 \end{cases} \tag{24}$$

$$h(x \Big/ \theta) = \begin{bmatrix} p(y=1|x,\ \theta) \\ p(y=2|x,\ \theta) \\ \cdots \\ p(y=k|x,\ \theta) \end{bmatrix} = \frac{1}{\sum_j \exp(\theta_j^T x)} \begin{bmatrix} \exp(\theta_1^T x) \\ \exp(\theta_2^T x) \\ \cdots \\ \exp(\theta_k^T x) \end{bmatrix} \tag{26}$$

By iterative optimization procedure, the value of θ can be estimated on the loss function.

Algorithm 4:

Pseudo code of DNN-ASCCS

Input: number of neurons, number of hidden layers and the number of input and output layers and dataset to train
Output: the best optimal solution
Initialize the populations of ASCCS algorithm
Compute the location of crows and initialize the memory for each crow
while the termination condition of the iteration is not satisfied ***do***
evaluate the search agents and define the awareness probability
update the position using Eqn (24)
end while
construct DNN-ASCCS with the best individual
for $i = 1$ *to MaxIteration* ***do***
Training data is passing through the DNN layers
sigmoid and mapping function is computed using Eqns (19) & (20)
Loss form and cross entropy loss are calculated using Eqns (21) & (22)
From the output layer, the error is back propagated to all hidden layers
by updating their weight values using Eqn (25)
Softmax function is computed using (26)
end for

$$\xi(t) = \xi_{\max} - (\xi_{\max} - \xi_{\min})\ \frac{t}{N_iter} \tag{25}$$

Where, the awareness of the crow j is denoted as AP_i^t, the flight length of the crow i is defined as fl_i^t, and the position of hiding place of crow i is signified as m_i^t. The current position is denoted as X_i^t, the position of the best solution is represented as P_i^t, r_1 is the update direction, r_2 is the updating distance, r_3 makes a proper trade-off amongst underline or minimize the result of desalination for the finest solution by allocating arbitrary weight sand a sine or cosine movement is selected by r_4. The maximum number of iteration is denoted as N_iter, $\xi_{\max}$ and $\xi_{\min}$ are the maximum and minimum inertia weight, respectively. The search agents can travel in a dissimilar way to improve the other solutions which growths the exploration capability of the procedure. The last layer of DNN is a softmax classifier and its main aim is to categorize the learned features from DNN. Softmax is used as the activation function in this classifier. It can be considered as a multinomial logistic regression with output has represented by:

4. Results and discussions

The proposed (DNN-ASCCS) approach is implemented in python environment using LIDC-IDRI datasets. The different performance metrics are estimated and compared to the existing classifiers and different state-of-art methods. The different classifiers [33] such as SVM,KNN, Naïve Bayes (NB), bagging and AdaBoost are utilized for the detection of lung cancer. By this analysis, the best classifier for lung cancer diagnosis is identified. To find the better accuracy, the k-fold cross-validation is used for LIDC-IDRI datasets. The total datasets are separated into k subgroups of data. A single subset is used as the test data and remaining subsets are used as the training data for each validation. This process is repeated k times. In this work, $k = 10$ is used to analyse the developed approach.

4.1. Dataset description

The LIDC-IDRI dataset is collected from The Cancer Imaging Archive

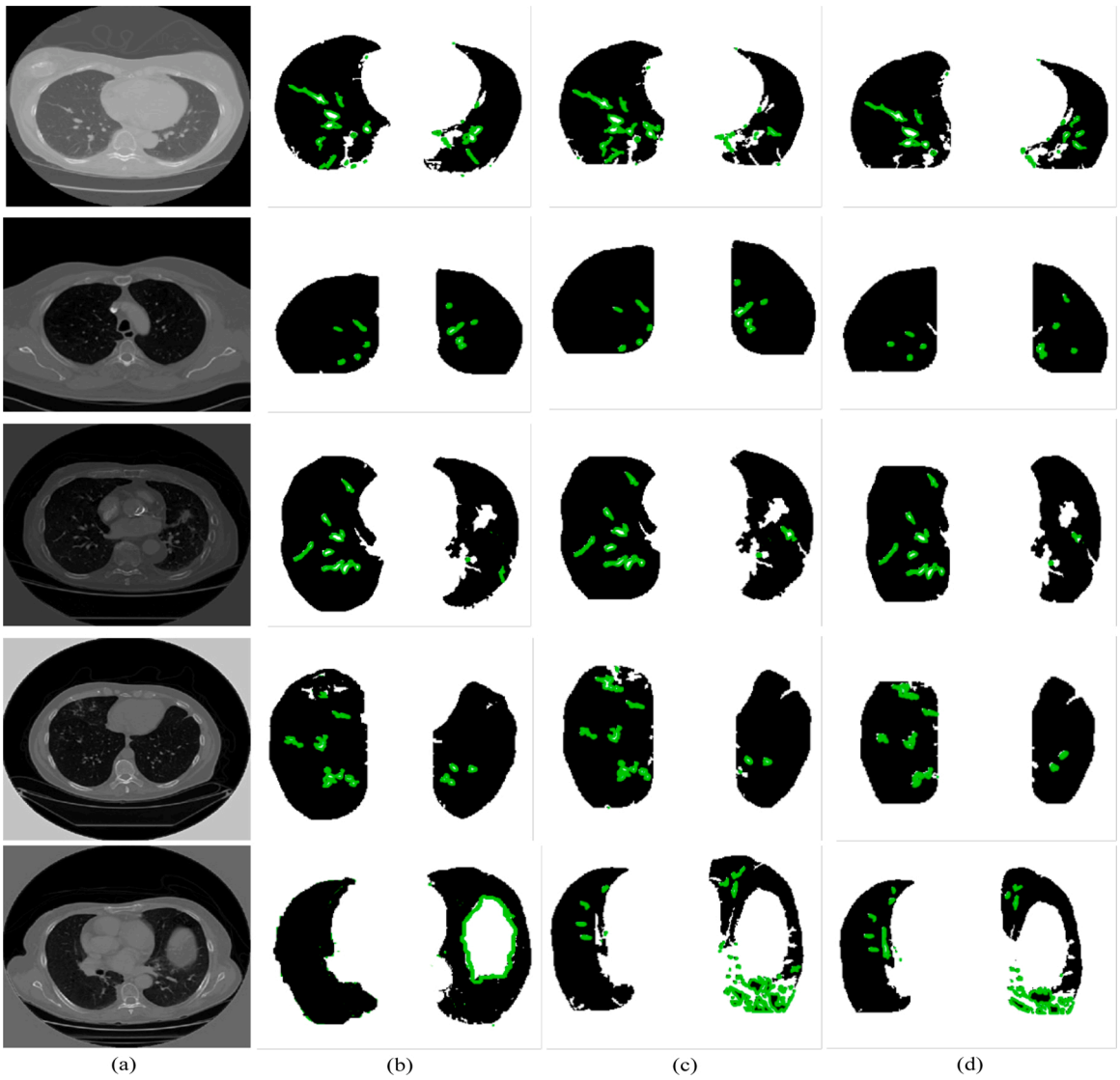


Fig. 4. (a) pre-processed images, (b) segmentation using MasiEMT-SSA, (c) segmentation using massi entropy (d) segmentation using region growing.

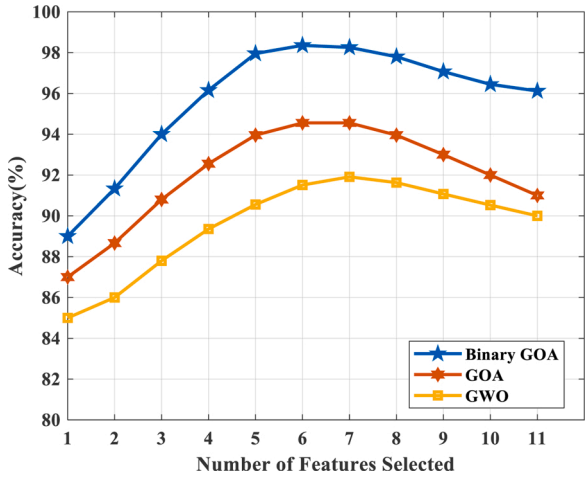


Fig. 5. Comparison of accuracy performance for different feature selection approaches.

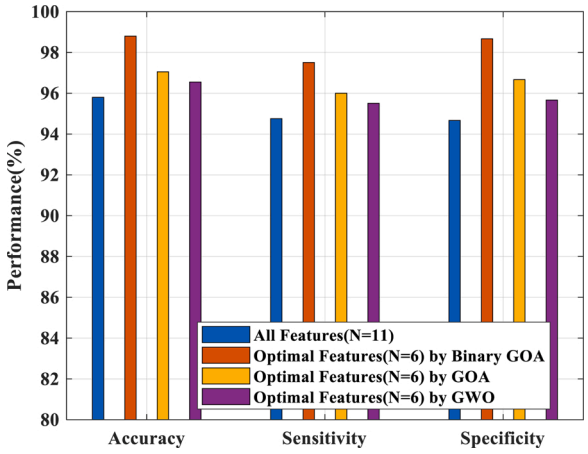


Fig. 6. Different performances for different feature selection approaches using all features and optimal features.

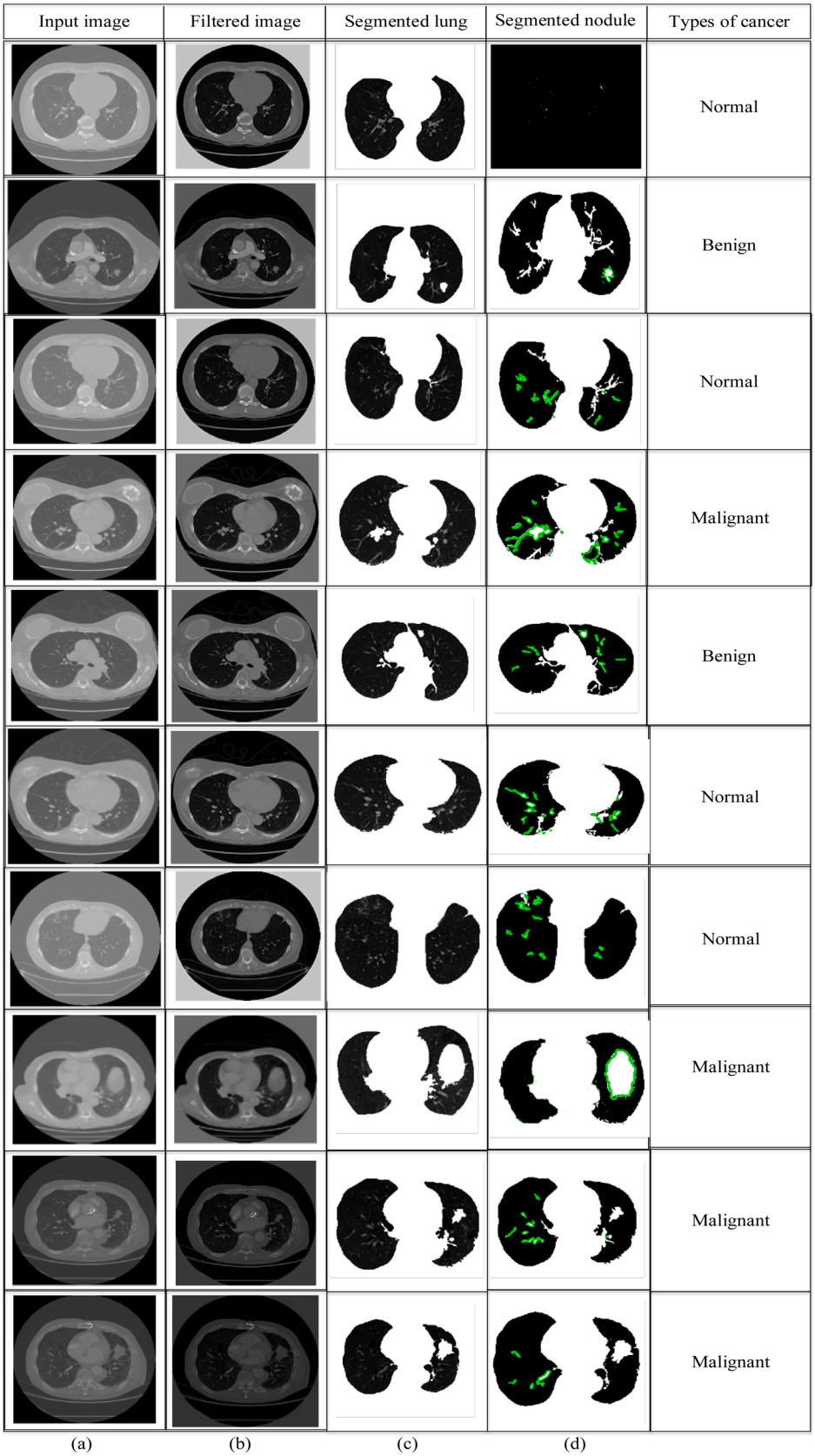


Fig. 7. Lung cancer output images (a) input image (b) filtered image (c) segmented lung (d) segmented nodule.

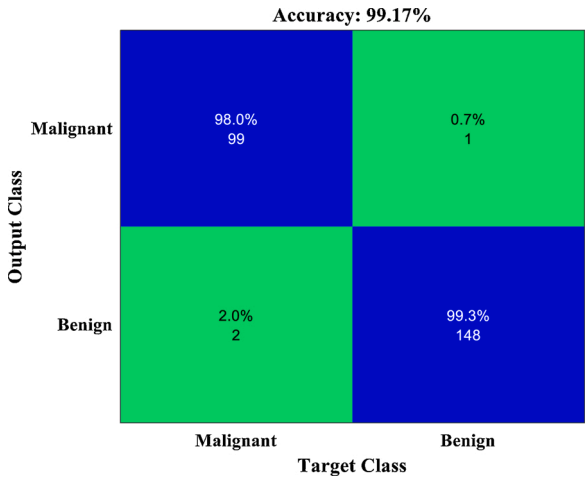


Fig. 8. Confusion matrix.

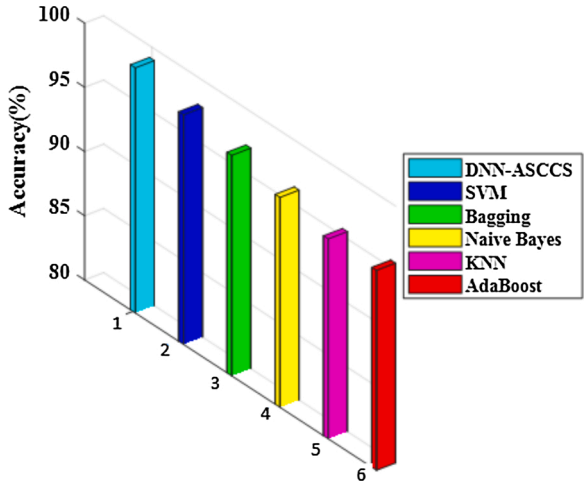


Fig. 9. Accuracy performance.

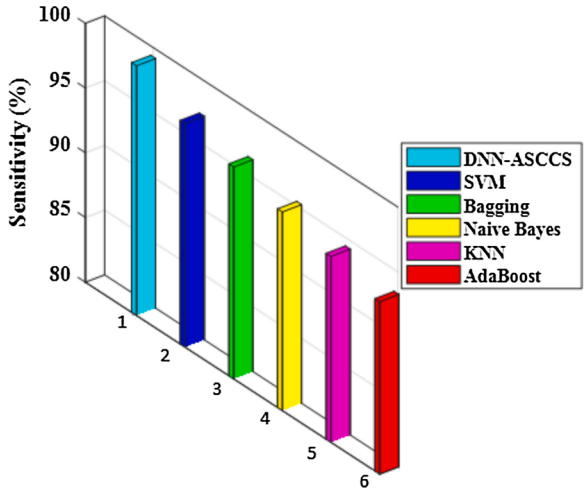


Fig. 10. Comparison of Sensitivity.

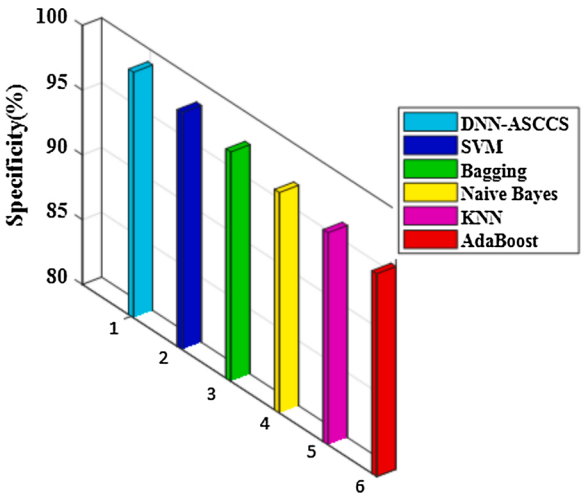


Fig. 11. Specificity evaluation.

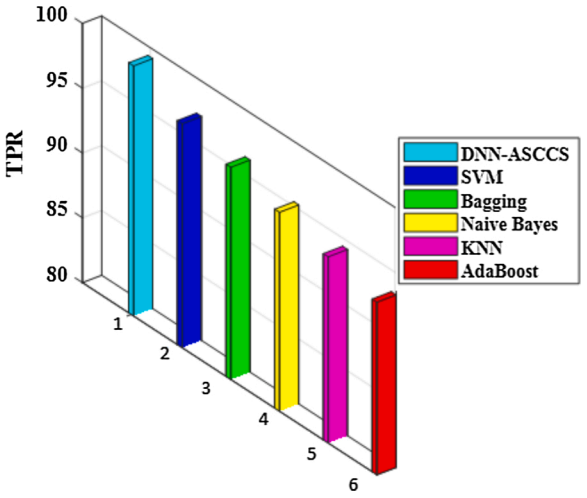


Fig. 12. TPR performance.

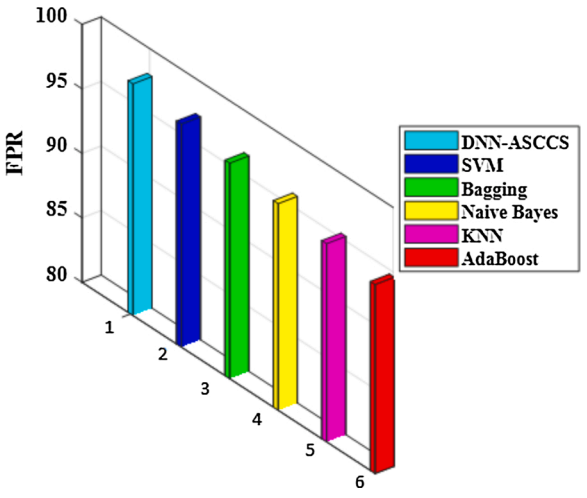


Fig. 13. FPR performance.

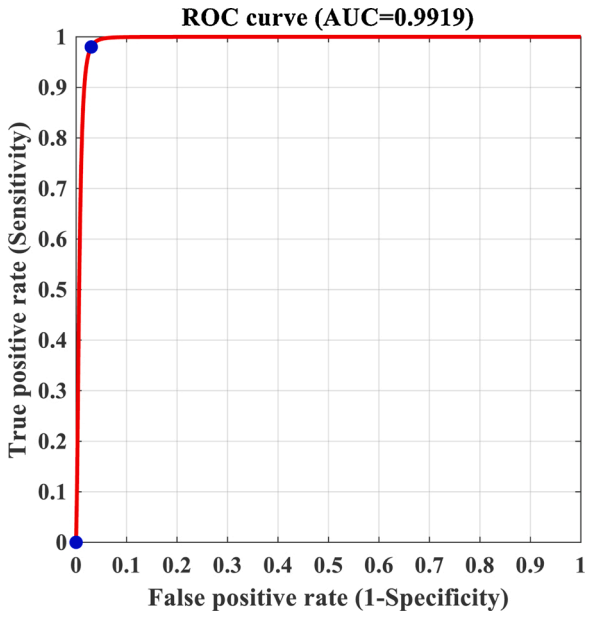


Fig. 14. ROC plot for DNN-ASCCS.

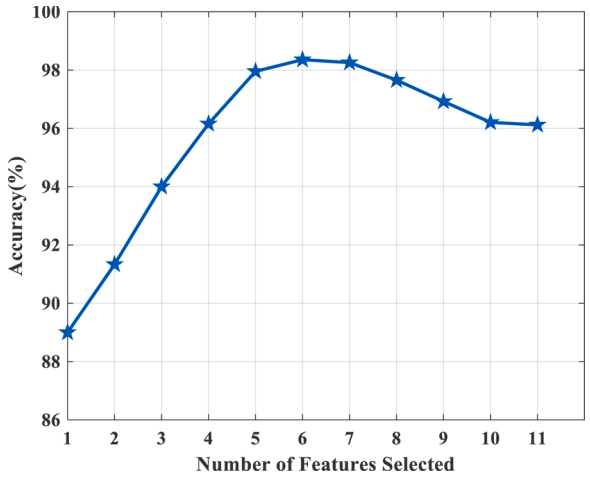


Fig. 15. Accuracies of different features.

(TCIA). The dataset consists of 1018 CT scans of 1010 patients. With the pixel size ranges between 0.48 and 0.72 mm, the thickness of each slice varies from 1.25 to 2.5 mm range. In this work, 70 % is used for training and 30 % is used for testing purposes. A comprehensive explanation of the LIDC-IDRI can be found in [34].

4.2. Performance metrics

In the proposed approach, different performance metrics are utilized for the diagnosis of lung cancer. They are accuracy, specificity, sensitivity, false positive and negative rate. Confusion matrix corresponding to true negative, false positive, true positives, and false negative is utilized for measuring the above parameters of the classifier. The following formulas define each of the metrics,

True Positive (TP): The mined dataset covering cancer nodule is categorized as cancerous

True Negative (TN): The mined dataset without cancer nodule is categorized as non-cancerous

False Positive (FP): The mined dataset without cancer nodule is categorized as cancerous

False Negative (FN): The mined dataset covering cancer nodule is categorized as non-cancerous

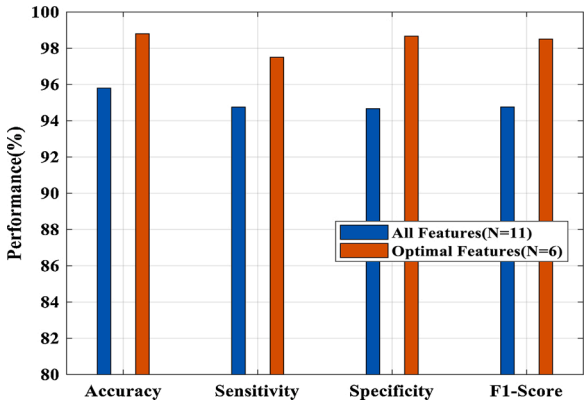


Fig. 16. Comparison of accuracy for LIDC-IDRI dataset before and after applying feature selection process.

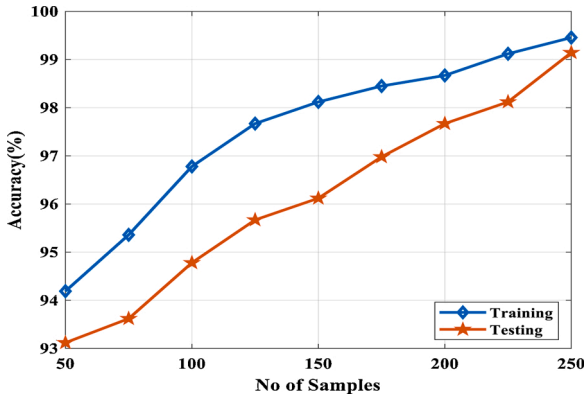


Fig. 17. Testing and training accuracy for the proposed method.

Table 1
Comparison of proposed approach with different classifiers.

Parameters	Acc (%)	Sensitivity (%)	Specificity (%)	TPR	FPR
DNN-ASCCS (proposed)	99.17	99.3	99.03	99.3	0.96
AdaBoost	94.77	93.3	95.7	93.3	4.29
KNN	95.5	94.3	96.3	94.3	3.68
NB	96.3	95.3	97.03	95.3	2.96
Bagging	97.11	96.3	97.64	96.3	2.35
SVM	97.88	97.28	98.28	97.28	1.72

Accuracy: It defined as how many samples were corrected accurately among the total number of samples and it is given as:

$$Acc = \frac{TP + TN}{TP + TN + FP + FN} \tag{27}$$

Sensitivity: It is predicting the positive values to actual positive values.

$$Sensitivity = \frac{TP}{TP + FN} \tag{28}$$

Specificity: It is a measurement of predicting actual negatives as negative.

$$Specificity = \frac{TN}{TN + FP} \tag{29}$$

False positive rate (FPR): It is the fraction of negative cases imperfectly identified as positive cases in the data.

Table 2
Computation for different steps of the proposed method.

Processing Steps	FNLM Filter (sec)	MasiEMT-SSA Segmentation (sec)	GLRLM Feature Extraction (sec)	BGOA Feature Selection (sec)	Classification (sec)	Total Time (sec)
DNN	1.83	7.14	32.61	50.75	42.23	134.56
DNN-ASCCS	1.83	7.14	32.61	50.75	15.67	108

Table 3
Comparison of different state-of-art methods with the proposed approach.

Authors	Classifiers	Datasets	Accuracy (%)
DNN-ASCCS (proposed)	DNN-ASCCS	LIDC-IDRI	99.17
Suresh [33]	DCNN	LIDC-IDRI	97.80
Lakshmanaprabu [35]	MGSA	LIDC-IDRI	94.56
de Carvalho Filho et al. [36]	CNN	LIDC-IDRI	92.63
Xie et al [37]	Fuse-TSD	LIDC-IDRI	89.53
Shen et al [38]	SVM, RF	LIDC-IDRI	86.84
Xie et al [39]	DCNN	LIDC-IDRI	92.53
Harikumar and Sannasi [40]	PNN	LIDC-IDRI	90

$$FPR = \frac{FP}{FP + TN} \tag{30}$$

False negative rate (FNR): It is the ratio of positive cases inaccurately identified as negative cases in the data.

$$FNR = \frac{FN}{FN + TP} \tag{31}$$

4.3. Performance analysis

4.3.1. Preprocessing

Fig. 3 shows the comparison of different preprocessing approaches of FNLM, robust bilateral filter, and rolling guidance filter. The proposed method using the FNLM filter for the preprocessing stage to remove the noise from the input images. The output pre-processed image using FNLM filter is compared to the existing filtering methods of rolling guidance filter and robust bilateral filter. FNLM filter provide the better quality image compared to other existing filtering approaches.

4.3.2. Segmentation

For an image segmentation process, a multilevel thresholding (MT) method is established that uses the Masi entropy as an impartial function. The complexity of MT is growths quickly with growing number of thresholds. In this algorithm, the population is divided into two groups such as leaders and followers. Fig. 4 displays the segmentation outputs using the MasiEMT-SSA, massi entropy and region growing approaches. The proposed scheme using the MasiEMT-SSA approach to segment the nodule from the lung images. The output segmented images compared to other existing segmentation approaches of region growing and massi entropy methods. The MasiEMT-SSA method accurately extracts the segmented portion from the lung images compared to the existing segmentation methods. The infected areas are denoted as green color in the segmented image using the MasiEMT-SSA algorithm with its adequate dimensions of segmentation.

4.3.3. Feature selection

Fig. 5 shows the accuracy performance comparison using different feature selection approaches. The proposed scheme using the BGOA method for feature selection and it compared to other existing feature selection methods of GOA and GWO. The BGOA method obtained the high accuracy for each features compared to other feature selection approaches. Each feature selection method obtained better accuracy for six optimal feature selection approaches. But the proposed scheme obtained high performance compared to other approaches.

Fig. 6 shows the different performance metrics comparison for different feature selection approaches using optimal features and all features. Accuracy, sensitivity and specificity values are obtained the lowest performance for all features. But optimal features provides the best performances for the BGOA compared to the existing feature selection approaches of GOA and GWO. Moreover, compared to the all features, the optimal features provide the best values for all performances such as accuracy, sensitivity and specificity.

4.3.4. Classification

The proposed (DNN-ASCCS) approach is performed using LIDC-IDRI datasets. The proposed scheme accurately identifies the lung cancer whether it is cancerous or non-cancerous. Initially, the images are converted into the gray scale images. Then the FNLM filter is used to remove the noise present in the images. Using MasiEMT-SSA is used to segment the lung nodule from the pre-processed image. After segmentation, GLRLM feature is extracted in the feature extraction process. BGOA is used to select the significant features which enhance the classification accuracy. After feature selection process, the selected features are provided to the DNN-ASCCS classifier to identify the lung cancer whether it is cancerous or non-cancerous. The different performance metrics are evaluated and compared to the existing classifiers and the different state-of-art methods. From the analysis, the proposed (DNN-ASCCS) is obtained the best performance compared to other approaches. The input image, and filtered image are shown in Fig. 7 (a) and (b). The segmented lung and segmented nodule are shown in Fig. 7 (c) and (d).

Fig. 8 shows the confusion matrix of proposed scheme. The DNN-ASCCS approach correctly identified the lung cancer whether it is cancerous or non-cancerous. The testing dataset contains 100 malignant images and 150 benign images. In the 100 malignant, only 99 images correctly identified as a malignant and remaining one is wrongly identified as a benign. The corrected malignant images (99) are given the 98 % Acc and the wrongly predicted malignant image (1) is provide the 0.7 % Acc. In the 150 benign, only 148 images are correctly identified as a benign and remaining two is wrongly identified as a malignant. The corrected benign images (148) are given the 99.3 % Acc and the wrongly predicted benign image (2) is provide the 2% Acc. The developed approach is provided the high classification accuracy (99.17 %) compared to the existing classifiers and other state-of-art methods.

Fig. 9 shows the accuracy performance of the proposed (DNN-ASCCS) approach and existing classifiers. The above graph clearly denotes that the proposed method is improved than other classifiers. The proposed scheme achieved the high classification accuracy (99.17 %) compared to the existing classifiers such as AdaBoost, KNN, NB, Bagging and SVM. The accuracy of existing classifier is 94.77 % for AdaBoost, 95.5 % for KNN, 96.3 % for NB, 97.11 % for bagging and 97.88 % for SVM. From these analysis, the proposed (DNN-ASCCS) approach is the best selection for the diagnosis of the lung cancer.

Fig. 10 shows the Sensitivity performance of the proposed (DNN-ASCCS) approach and existing classifiers. The above graph clearly denotes that the proposed method is improved than other classifiers. The proposed scheme achieved the high Sensitivity (99.3 %) compared to the existing classifiers such as AdaBoost, KNN, NB, Bagging and SVM. The sensitivity of existing classifier is 93.3 % for AdaBoost, 94.3 % for KNN, 95.3 % for NB, 96.3 % for bagging and 97.28 % for SVM. From these analysis, the proposed (DNN-ASCCS) approach is the best selection for the diagnosis of the lung cancer.

Fig. 11 shows the Specificity performance of the proposed (DNN-ASCCS) approach and existing classifiers. The above graph clearly denotes that the proposed method is improved than other classifiers. The

proposed scheme achieved the high Specificity (99.03 %) compared to the existing classifiers such as AdaBoost, KNN, NB, Bagging and SVM. The specificity of existing classifier is 95.7 % for AdaBoost, 96.3 % for KNN, 97.03 % for NB, 97.6 % for bagging and 98.28 % for SVM. From this analysis, the proposed (DNN-ASCCS) approach is the best selection for the diagnosis of the lung cancer.

Fig. 12 shows the TPR performance of the proposed (DNN-ASCCS) approach and existing classifiers. The above graph clearly denotes that the proposed method is improved than other classifiers. The proposed scheme achieved the high TPR (99.3 %) compared to the existing classifiers such as AdaBoost, KNN, NB, Bagging and SVM. The TPR of existing classifier is 93.3 for AdaBoost, 94.3 for KNN, 95.3 for NB, 96.3 for bagging and 97.28 for SVM. From these analyses, the proposed (DNN-ASCCS) approach is the best selection for the diagnosis of the lung cancer.

Fig. 13 shows the FPR performance of the proposed (DNN-ASCCS) approach and existing classifiers. The above graph clearly denotes that the proposed method is improved than other classifiers. The proposed scheme achieved the low FPR (0.96) compared to the existing classifiers such as AdaBoost, KNN, NB, Bagging and SVM. The FPR of existing classifier is 4.29 for AdaBoost, 3.68 for KNN, 2.96 for NB, 2.35 for bagging and 1.72 for SVM. From these analyses, the proposed (DNN-ASCCS) approach is the best selection for the diagnosis of the lung cancer.

Fig. 14 shows the ROC curve of the proposed (DNN-ASCCS) method. A measure of discriminatory performance for the specific model is termed as ROC (receiver operating curve) and it calculating the area which is under the curve. The wide-ranging accessibility of computer software to calculate the area under the curve so the ROC developed more popular in current decades. ROC is a plot of sensitivity by 1-specificity values which obtained from classification method utilized to categorize the datasets as benign and malignant. The proposed (DNN-ASCCS) obtained high rate (0.99) which proves that the DNN-ASCCS classifier is best scheme for the lung cancer diagnosis.

Fig. 15 shows the classification accuracy for different features using LIDC-IDRI datasets. DNN-ASCCS needs a certain number of features to be kept, but the number of valid features that DNN-ASCCS needs is not known in advance. Thus, to know the exact number of features required, the fitness of each feature is used to score different feature subsets and get the best and the most optimal collection of features. The above graph visualizes how the number of features selected. From the graph, the six features are only given best accuracy for LIDC-IDRI datasets.

Fig. 16 shows the comparison accuracy for all features and selected features using LIDC-IDR dataset. If all features are directly given to the classification process, then the classification accuracy is decreases and also execution time increased. For this reason, the BGOA approach is used to select the optimal features and it given to the classification purpose. The feature selection process reduce the processing time and improves the accuracy performance. The proposed method gives the better accuracy for optimal features. GLRLM contains 11 features. In this work, only 6 features are selected using BGOA which were noteworthy for lung cancer diagnosis. From the analysis, the proposed scheme provide the best accuracy with reduced number of features for LIDC-IDRI dataset compared to other classifiers.

Fig. 17 shows the classification accuracy for testing and training images. The accuracy for training and testing is increases with the number of samples increases. The training images obtained the high accuracy compared to the testing images. The proposed method obtained the high classification accuracy than existing classifiers.

Table 1 shows the comparison of different performance metrics for the proposed (DNN-ASCCS) approach and existing classifiers of AdaBoost, KNN, NB, Bagging and SVM. The proposed method obtained the high classification accuracy (99.17 %), sensitivity is 99.3 %, specificity is 99.03 %, TPR is 99.3 and FPR is 0.96 compared to the existing classifiers. The accuracy of existing classifier is 94.77 % for AdaBoost, 95.5 % for KNN, 96.3 % for NB, 97.11 % for bagging and 97.88 % for SVM. From these analyses, the proposed (DNN-ASCCS) approach is greatly improved in all performance metrics compared to other classifiers for the LIDC-IDRI dataset.

4.3.4.1. Computation time analysis. Computation time is the amount of time taken by the system to obtain the required results. The work uses Intel Core i3 II generation processor based 4 GB RAM computer with MATLAB 2018a environment. The obtained computation times on running the corresponding program for both the techniques are given in Table 2 where classification using DNN classifier and hybrid DNN with ASCCS classifier. It is seen that the computation time of DNN-ASCCS is almost very less computation time of DNN. Table 2 shows the run time of each processing steps in our proposed method. It took total simulation time about 134.56 s of DNN classifier whereas 108 s for DNN –ASCCS classifier. The proposed DNN-ASCCS Classification execution time is 15.67 s but DNN classification execution time is 42.23 s. The robustness of DNN and higher convergence property of ASCCS towards the output classes make the proposed model to perform well better in both the aspect of accuracy and the time taken for computation.

Table 3 shows the comparison accuracy of different state-of-art methods with the proposed scheme. From this table, the proposed scheme obtained the best accuracy for LIDC-IDRI dataset compared to the existing methods.

So far performance analysis displays that the proposed method is superior using LIDC-IDRI dataset compared to the existing classifiers and different state-of-art methods. The comparison performance metrics of accuracy, sensitivity, specificity, FPR, and FNR is better for the proposed approach compared to the existing approaches. Form these results, we have stated that the proposed (DNN-ASCCS) approach is best selection for the diagnosis of lung cancer.

5. Conclusions

The death rate can be decreased by the diagnosis of early lung cancer. But there is lot of difficulty in the discovery of early lung tumour classification. In this paper, a diagnosis of lung cancer using hybrid deep neural network with adaptive optimization procedure has been proposed. The main goal of this paper is to distinguish the malignant lung nodules and to categorize the lung tumour whether it is malignant or benign. The different processes like preprocessing, segmentation, feature extraction, feature selection and classification are performed for the lung cancer detection. At first, the preprocessing stage is performed using the FNLM filter. Then the MasiEMT-SSA approach is used to segment the cancer nodule from the lung images for the segmentation. In the feature extraction, different features are extracted by GLRLM approach from the segmented images. After the feature extraction stage, the feature selection stage is performed using the BGOA algorithm. It effectively chooses the optimal features from all the features. Then the designated features are provided to the hybrid classifier termed as DNN-ASCCS. Here, DNN is employed for the classification process and softmax regression is used in the output layer of DNN which is employed to categorize the lung tumour. In this classification procedure, the ASCCS algorithm is used for the weight calculation of DNN. The proposed (DNN-ASCCS) scheme is implemented in the MATLAB environment using LIDC-IDRI datasets. The simulation outcomes verified that the DNN-ASCCS approach provides the best results in all performance metrics related to the other classifiers and

different state-of-art methods. In the future, the proposed approach will be extended by the diagnosis of lung cancer using advanced methods and algorithms in less time complexity.

Author's contribution

PS contributed to technical and conceptual content, architectural design.MP contributed to guidance and counselling on the writing of the paper.

Human and animal rights

There is no animal involvement in this research.

Informed consent

The authors declare that they have no consent.

Declaration of Competing Interest

The authors report no declarations of interest.

References

[1] Amit Kumar, Fahimuddin Shaik, B. Abdul Rahim, D. Sravan Kumar, Signal and Image Processing in Medical Applications, Springer, Singapore, 2016.
[2] Sabah N. Mazhir, AlyaaH. Ali, Farah W. Hadi, AlaaN. Mazher, Studying the effect of dielectric barrier discharges on the leukemia blood cells using digital image processing, IOSR J. Pharm. Biol. Sci. 12 (2) (2017) 6–12.
[3] M.Parisa Beham, A.B. Gurulakshmi, Morphological image processing approach on the detection of tumor and cancer cells, in: 2012 International Conference on Devices, Circuits and Systems (ICDCS), IEEE, 2012, pp. 350–354.
[4] David Gutman, Noel C.F. Codella, BrianHelba EmreCelebi, Michael Marchetti, Nabin Mishra, Allan Halpern, Skin Lesion Analysis Toward Melanoma Detection: a Challenge at the International Symposium on Biomedical Imaging (ISBI) 2016, Hosted by the International Skin Imaging Collaboration (ISIC), arXiv preprint arXiv:1605.01397, 2016.
[5] Global Burden of Disease Cancer Collaboration, The global burden of cancer 2013, JAMA Oncol. 1 (4) (2015) 505.
[6] Neelima Singh, A. Asuntha, Lung cancer detection using medical images through image processing, Chem 9 (3) (2016).
[7] S.J. Sushma, S.C. Prasanna Kumar, Advancement in research techniques on medical imaging processing for breast cancer detection, Int. J. Electr. Comput. Eng. 6 (2) (2016) 717.
[8] Gunes Gundem, Peter Van Loo, Barbara Kremeyer, LudmilB. Alexandrov, Jose M. C. Tubio, Elli Papaemmanuil, Daniel S. Brewer, et al., The evolutionary history of lethal metastatic prostate cancer, Nature 520 (7547) (2015) 353.
[9] T. Luca, V. Barresi, G. Privitera, N. Musso, M. Caruso, D.F. Condorelli, S. Castorina, In vitro combined treatment with cetuximab and trastuzumab inhibits growth of colon cancer cells, Cell Prolif. 47 (5) (2014) 435–447.
[10] James L. Devin, Michelle M. Hill, Marina Mourtzakis, Joe Quadrilatero, David G. Jenkins, Tina L. Skinner, Acute high intensity interval exercise reduces colon cancer cell growth, J. Physiol. 597 (8) (2019) 2177–2184.
[11] Ahmed M. Anter, AboulElla Hassenian, Computational intelligence optimization approach based on particle swarm optimizer and neutrosophic set for abdominal CT liver tumor segmentation, J. Comput. Sci. 25 (2018) 376–387.
[12] Tharcis Paulraj, KeziS.V. Chellliah, Computer-Aided Diagnosis of lung cancer in Computed Tomography scans: A Review, Curr. Med. Imaging Rev. 14 (3) (2018) 374–388.
[13] Nicholas Petrick, Berkman Sahiner, Samuel G. Armato III, Alberto Bert, Loredana Correale, Silvia Delsanto, Matthew T. Freedman, et al., Evaluation of computer-aided detection and diagnosis systems a, Med. Phys. 40 (8) (2013), 087001.
[14] Emilie L. Henriksen, Jonathan F. Carlsen, Ilse M.M. Vejborg, Michael B. Nielsen, Carsten A. Lauridsen, The efficacy of using computer-aided detection (CAD) for detection of breast cancer in mammography screening: a systematic review, ActaRadiologica 60 (1) (2019) 13–18.
[15] T. Manikandan, N. Bharathi, M. Sathish, V. Asokan, Hybrid neuro-fuzzy system for prediction of lung diseases based on the observed symptom values, J. Chem. Pharm. Sci. ISSN 974 (2017) 2115.
[16] Neha Malviya, Naveen Choudhary, Kalpana Jain, Content based medical image retrieval and clustering based segmentation to diagnose lung cancer, Adv. Comput. Sci. Technol. 10 (6) (2017) 1577–1594.
[17] Jeyaprakash Vasanth Wason, Ayyappan Nagarajan, Image processing techniques for analyzing CT scan images towards the early detection of lung cancer, Bioinformation 15 (8) (2019) 596–599.
[18] Shehzad Khalid, Uzma Jamil, Valuable Pre-Processing and Segmentation Techniques Used in Automated Skin Lesion Detection Systems, 2015.
[19] Ahmad Chaddad, Automated feature extraction in brain tumor by magnetic resonance imaging using gaussian mixture models, J. Biomed. Imaging (2015) (2015) 8.
[20] YooNa Hwang, JuHwan Lee, Ga Young Kim, YuanYuan Jiang, Sung Min Kim, "Classification of focal liver lesions on ultrasound images by extracting hybrid textural features and using an artificial neural network, Biomed. Mater. Eng. 26 (s1) (2015) S1599–S1611.
[21] R. Arulmurugan, H. Anandakumar, Early detection of lung cancer using wavelet feature descriptor and feed forward back propagation neural networks classifier. Computational Vision and Bio Inspired Computing, Springer, Cham, 2018, pp. 103–110.
[22] A.P.Ayshath Thabsheera, T.M. Thasleema, R. Rajesh, Lung cancer detection using CT scan images: a review on various image processing techniques. Data Analytics and Learning, Springer, Singapore, 2019, pp. 413–419.
[23] Haixin Yu, Zhong Guan, Katarina Cuk, Yan Zhang, Hermann Brenner, Circulating MicroRNA biomarkers for lung cancer detection in east asian populations, Cancers 11 (3) (2019) 415.
[24] Ananya Bhattacharjee, Swanirbhar Majumder, Automated computer-aided lung cancer detection system. Advances in Communication, Devices and Networking, Springer, Singapore, 2019, pp. 425–433.
[25] Yochai Adir, Shoval Tirman, Shirley Abramovitch, Cynthia Botbol, Aviv Lutaty, Tali Scheinmann, Eyal Davidovits, et al., Novel non-invasive early detection of lung cancer using liquid immunobiopsy metabolic activity profiles, Cancer Immunol. Immunother. 67 (7) (2018) 1135–1146.
[26] Jina Shim, Myonggeun Yoon, Youngjin Lee, Quantitative study of fast non-local means-based denoising filter in chest X-ray imaging with lung nodule using three-dimensional printing, Optik 179 (2019) 1180–1188.
[27] AbdulKayomMd Khairuzzaman, Saurabh Chaudhury, Masi entropy based multilevel thresholding for image segmentation, Multimed. Tools Appl. 78 (23) (2019) 33573–33591.
[28] Seyedali Mirjalili, Amir H. Gandomi, SeyedehZahra Mirjalili, Shahrzad Saremi, Hossam Faris, SeyedMohammad Mirjalili, Salp Swarm Algorithm: A bio-inspired optimizer for engineering design problems, Adv. Eng. Softw. 114 (2017) 163–191.
[29] Telagarapu Prabhakar, KilpattuRamaniharan Anandh, Annapantula Sudhakar, Classification of Alzheimer's condition in T1-weighted MR images using GLCM and GLRLM texture features, in: Proceedings of International Conference on Wireless Communication, Springer, Singapore, 2020, pp. 533–541.
[30] Majdi Mafarja, Ibrahim Aljarah, Hossam Faris, AbdelazizI. Hammouri, Al-ZoubiAla'M, Seyedali Mirjalili, Binary grasshopper optimisation algorithm approaches for feature selection problems, Expert Syst. Appl. 117 (2019) 267–286.
[31] Seyedali Mirjalili, SCA: a sine cosine algorithm for solving optimization problems, Knowledge Based Syst. 96 (2016) 120–133.
[32] Alireza Askarzadeh, A novel metaheuristic method for solving constrained engineering optimization problems: crow search algorithm, Comput. Struct. 169 (2016) 1–12.
[33] Supriya Suresh, Subaji. Mohan, NROI based feature learning for automated tumor stage classification of pulmonary lung nodules using deep convolutional neural networks, J. King Saud Univ. - Comput. Inf. Sci. (2019), https://doi.org/10.1016/j.jksuci.2019.11.013.
[34] LIDC-IDRI. [Online] https://wiki.cancerimagingarchive.net/display/Public/LIDC-IDRI.
[35] S. Lakshmanaprabu, S.N. Mohanty, K. Shankar, N. Arunkumar, G. Ramirez, Optimal deep learning model for classification of lung cancer on ct images, Future Gener. Comput. Syst. 92 (2019) 374–382.
[36] A.O. de Carvalho Filho, A.C. Silva, A.C. de Paiva, R.A. Nunes, M. Gattass, Classification of patterns of benignity and malignancy based on ct using topology-based phylogenetic diversity index and convolutional neural network, Pattern Recognit. 81 (2018) 200–212.
[37] Y. Xie, J. Zhang, Y. Xia, M. Fulham, Y. Zhang, Fusing texture, shape and deep model-learned information at decision level for automated classification of lung nodules on chest ct, Inf. Fusion 42 (2018) 102–110.
[38] W. Shen, M. Zhou, F. Yang, C.Y. Yang, J. Tian, Multi-scale convolutional neural networks for lung nodule classification, in: Information Processing in Medical Imaging, Springer: Cham, Switzerland, 2015, pp. 588–599.
[39] Y. Xie, J. Zhang, Y. Xia, Semi-supervised adversarial model for benign–malignant lung nodule classification on chest CT, Med. Image Anal. 57 (2019) 237–248.

[40] S.R. Sannasi Chakravarthy, Harikumar Rajaguru, Lung cancer detection using probabilistic neural network with modified crow-search algorithm, Asian Pacific J. Cancer Prevention: APJCP 20 (7) (2019) 2159.
[41] Yu-Dong Zhang, Suresh Satapathy, David Guttery, Juan Gorriz, Shuihua Wang, Improved breast cancer classification through combining graph convolutional network and convolutional neural network, Inf. Process. Manag. 58 (2021) 102439, https://doi.org/10.1016/j.ipm.2020.102439.
[42] Shuihua Wang, Vishnuvarthanan Govindaraj, Juan Gorriz, Xin Zhang, Yu-Dong Zhang, Covid-19 classification by FGCNet with deep feature fusion from graph convolutional network and convolutional neural network, Inf. Fusion (2020), https://doi.org/10.1016/j.inffus.2020.10.004.



P. Surendar is working as an Assistant Professor in Electronics and Communication Engineering, in Vivekanandha College of Engineering for Women, Namakkal. He completed his Post graduation in Applied Electronics in the year 2011. He worked as an Assistant Professor in M. Kumarasamy College of Engineering for 5 Years. His Area of interest is Medical Image Processing and doing research work in this field. Having good skill in Image Processing, he have Published some of his work in reputed Journals.



Dr. M. Ponni Bala is working as Associate Professor in Electronics and Instrumentation Engineering, Kongu Engineering College, Erode. She received her PhD degree in Information and Communication from the Anna University, Chennai. She received ME in Power Electronics BE degree in Electronics and Instrumentation from Anna University. She is. She has 17 years of teaching experience. Her research areas include Machine learning, Biomedical Image Processing, Soft computing. She act as a supervisor of 4 Research scholars, guided 58 under graduates and 25 Post Graduates engineering projects. She presented 12 papers in National Conferences and International Conferences and 10 papers in International Journals. She received 6 funded projects from CSIR, ICMR, DRDO and DBT.